In cooperation with
AVDC
AMERICAN VETERINARY DENTAL COLLEGE

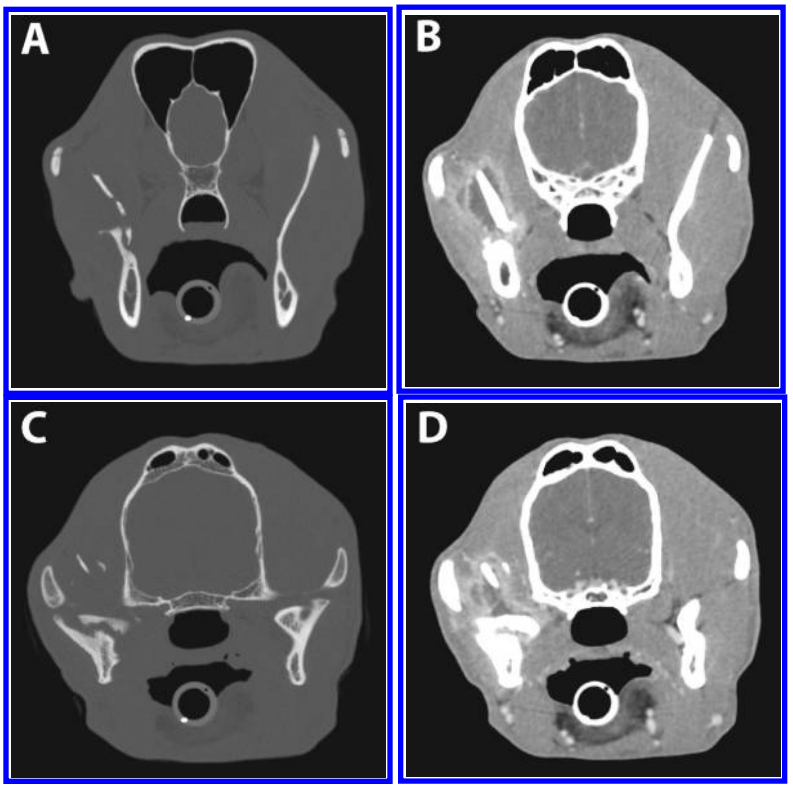

Figure 1—Representative transverse CT images of a 20-month-old English Springer Spaniel evaluated for recurrent extraoral swelling in the caudal left mandibular region and an intraoral draining tract. Images were obtained at the level of the mandibular rami (A and B) and condylar processes of the mandibles (C and D), before (A and C) and after (B and D) contrast medium administration. Unenhanced and contrast-enhanced images were viewed with bone (window width, 2,500 HU; window level, 480 HU) and soft tissue (window width, 350 HU; window level, 40 HU) settings, respectively.

History and Physical Examination Findings

A 20-month-old 18-kg (39.6-lb) spayed female English Springer Spaniel was referred to a veterinary medical teaching hospital (VMTH) for recurrent extraoral swelling in the caudal left mandibular region and an intraoral draining tract near the left mandibular ramus. Seven months earlier, the referring veterinarian evaluated the dog for left-sided facial swelling, oral bleeding, and signs of oral pain. Mild left-sided facial swelling, a suspected abscess in the caudal left pharyngeal area, and ipsilateral secretion of blood-tinged purulent saliva were observed. Enrofloxacin (3.8 mg/kg [1.7 mg/lb], PO, q 24 h for 10 days) was prescribed. Periodontal treatment and left mandibular second and third molar tooth extractions were performed 6 days later. Aerobic and anaerobic microbial cultures of suspected abscess samples yielded β-hemolytic *Streptococcus* spp, *Staphylococcus pseudintermedius*, *Peptostreptococcus* sp, and (unspecified) normal flora. Antimicrobial susceptibility testing was performed for only the *S pseudintermedius* isolate owing to the predictable effectiveness of recommended antimicrobials for other isolates. The *S pseudintermedius* isolate was penicillin and amoxicillin resistant.

The dog was seen and treated several times over the next 6 months **(Appendix)**. A left-sided oral draining tract was noted 2 months prior to the referral visit; skull radiography–contrast fistulography revealed the left mandibular ramus was shorter, with slightly irregular margination, and the left temporomandibular joint (TMJ) was less clearly defined than contralateral structures. The lateral margin of the left condylar process appeared mildly irregular, thickened, and sclerotic. One view of the left mandibular ramus revealed circular areas of decreased opacity or overlying gas. Contrast medium accumulated rostral to the left TMJ in the retrobulbar region and entered the oral cavity. One month later, the dog was treated again for persistent purulent oral discharge and referred to the VMTH.

At the VMTH, extraoral examination revealed mild left masseter muscle atrophy without facial swelling and mild left mandibular lymphadenomegaly. Intraoral examination revealed a 2-cm-diameter region of erythematous oral mucosa over the left mandibular ramus, with missing left mandibular second and third molar teeth. Mandibular range of motion was mildly decreased. Contiguous transverse 0.6-mm collimated CT images of the head with 3-D volume rendering were obtained under anesthesia before and after iopamidol[a] (370 mg/mL; 880 mg/kg [400 mg/lb], IV) administration **(Figure 1)**.

Determine whether additional studies are required, or make your diagnosis, then turn the page→

This report was submitted by Da Bin Lee, DVM; Katherine D. Watson, DVM, PhD; Sabrina Wilson, DVM; and Boaz Arzi, DVM; from the Dentistry and Oral Surgery Service (Lee), Anatomic Pathology Service (Watson), and Diagnostic Imaging Service (Wilson), William R. Pritchard Veterinary Medical Teaching Hospital, and the Department of Surgical and Radiological Sciences (Arzi), School of Veterinary Medicine, University of California-Davis, Davis, CA 95616.

Address correspondence to Dr. Arzi (barzi@ucdavis.edu).

Diagnostic Imaging Findings and Interpretation

Digital images were evaluated on a medical-grade flat-screen monitor by use of commercially available software.[b–d] Images were viewed with bone (window width, 2,500 HU; window level, 480 HU) and soft tissue (window width, 350 HU; window level, 40 HU) display settings. A comminuted fracture of the left mandibular ramus, including the condylar process (both in 1 segment), was observed **(Figures 2 and 3)**. All fragments had variable irregular to wispy periosteal proliferation without a bridging callus. The largest fragment was of the mandibular coronoid process connected to the condylar process and extending ventrally to the mandibular ramus; this fragment was surrounded by centrally fluid- to soft tissue–attenuating, non–contrast-enhancing structures with thick, irregularly margined contrast-enhancing rims consistent with abscess formation. The mandibular head on the condylar process and the articular surface of the mandibular fossa had irregular osseous proliferation and osteolysis consistent with osteomyelitis. There were a few small, hyperattenuating fragments medial and lateral to the main fragment. Additionally, multiple peripherally contrast-enhancing, centrally fluid- to soft tissue–attenuating structures were interspersed with and surrounded the fracture fragments, consistent with abscess formation. A thin extension of contrast enhancement to the left caudal region of the oral mucosa and soft tissue thickening were associated with the distal aspect of the mandibular coronoid process fragment, consistent with a draining tract extending toward the region of erythematous oral mucosal detected on visual examination. There was a large, mildly hyperattenuating articular fracture fragment of the medial aspect of the condylar process of the mandible that remained in close apposition to the zygomatic arch. Focal osseous proliferation extended from the laterocaudal aspect of the left retroarticular

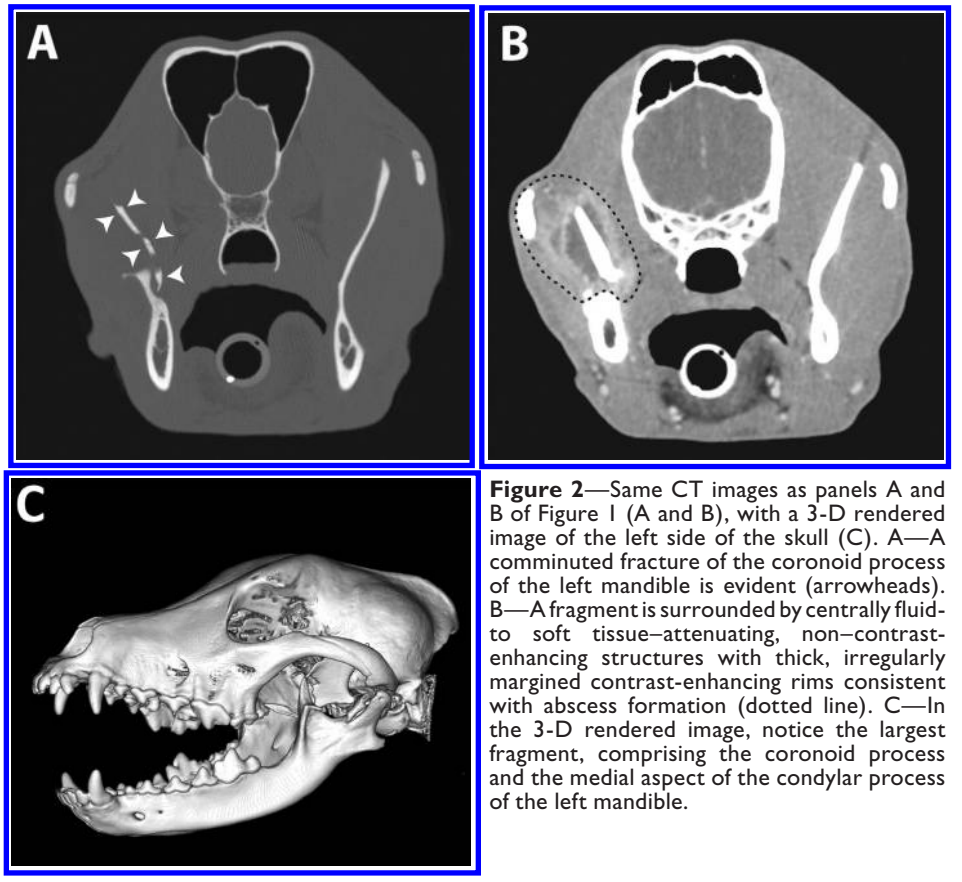

Figure 2—Same CT images as panels A and B of Figure 1 (A and B), with a 3-D rendered image of the left side of the skull (C). A—A comminuted fracture of the coronoid process of the left mandible is evident (arrowheads). B—A fragment is surrounded by centrally fluid- to soft tissue–attenuating, non–contrast-enhancing structures with thick, irregularly margined contrast-enhancing rims consistent with abscess formation (dotted line). C—In the 3-D rendered image, notice the largest fragment, comprising the coronoid process and the medial aspect of the condylar process of the left mandible.

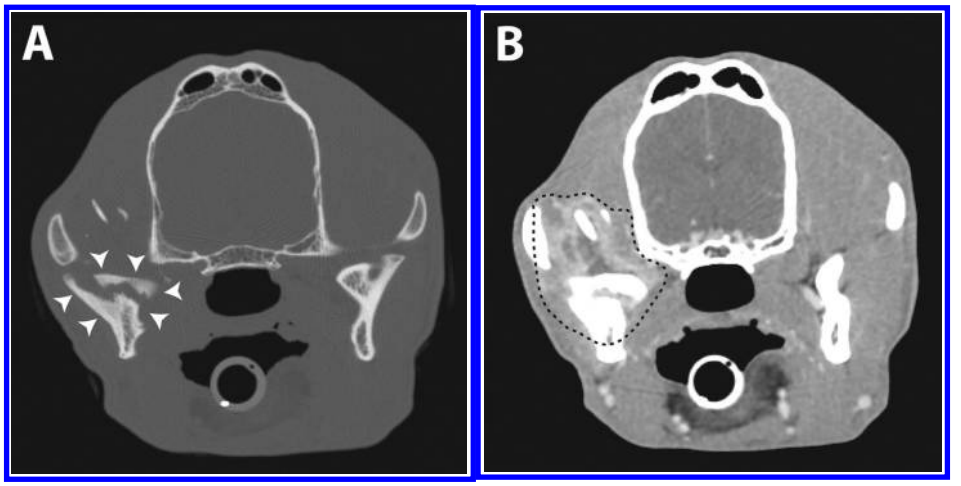

Figure 3—Same CT images as panels C and D of Figure 1. A—There is a fracture of the condylar process of the left mandible (arrowheads). B—The fracture fragment is surrounded by peripherally contrast-enhancing, centrally hypoattenuating structures, consistent with abscess formation as shown in panel B of Figure 2 (dotted lines). Additionally, the margins of the fracture fragment and parent condyle have irregular osteolysis and irregular periosteal proliferation.

process toward the abnormal left condylar process, which was concerning for development of ankylosis. The left parotid, left and right medial retropharyngeal, and left mandibular lymph nodes were enlarged and had foamy contrast enhancement, consistent with lymph node reactivity.

The CT diagnosis was a comminuted, chronic articular fracture of the left TMJ with osteomyelitis, septic arthritis, and regional abscess formation as well as regional lymph node reactivity. Three-dimensional reconstructed images allowed for better visualization of all fracture fragments, aiding surgical planning (Figure 2).

Treatment and Outcome

Left-sided zygomectomy and sequestrectomy were performed. Three fragments, the largest being of the coronoid process and including the medial aspect of the condylar process of the left mandible, were removed and submitted for aerobic and anaerobic culture and susceptibility testing as well as histopathologic analysis. Clindamycin phosphate (11 mg/kg [5 mg/lb], IV) was administered during surgery, and carprofen (2.2 mg/kg [1 mg/lb], IV) was administered once after surgery. A fentanyl patch (50 µg/h) was placed after surgery. The dog was discharged from the hospital, and the owner was instructed to administer carprofen (2.1 mg/kg [1 mg/lb], PO, q 12 h) and gabapentin (11.1 mg/kg [5 mg/lb], PO, q 8 to 12 h) for 7 to 10 days and to give amoxicillin–clavulanic acid (13.9 mg/kg [6.3 mg/lb], PO, q 12 h) until culture results were available. The owner was instructed to feed a soft diet for 1 week after surgery and then encourage the dog to use its jaw more by feeding large kibble and treats and inviting play with toys in an attempt to prevent ankylosis of the left TMJ.

The histopathologic diagnosis was severe, regionally extensive, suppurative osteomyelitis and periostitis with osteonecrosis, osteolysis, articular cartilage necrosis, and biofilm formation **(Figure 4)**. Culture yielded *Corynebacterium* sp, large amounts of mixed bacterial growth including *Peptostreptococcus anaerobius* and *Porphyromonas* sp, and 2 colony types of *Bacteroides* sp or *Prevotella* sp. Susceptibility testing was not performed by the microbiology service owing to the predictable effectiveness of the recommended antimicrobials. A veterinary microbiologist was consulted, and treatment with amoxicillin–clavulanic acid (13.9 mg/kg, PO, q 12 h) was continued for 4 weeks.

The dog was reevaluated 3 weeks after the surgery. The owners reported that the dog had substantially improved after surgery and was acting like itself again, with no signs of pain. Extraoral examination revealed bilateral temporalis muscle and left masseter muscle atrophy as well as mild left mandibular lymphadenomegaly. The dog had a perceived normal mandibular range of motion and a healed left zygomectomy incision site. The owners were instructed to complete the remaining course of amoxicillin–clavulanic acid treatment.

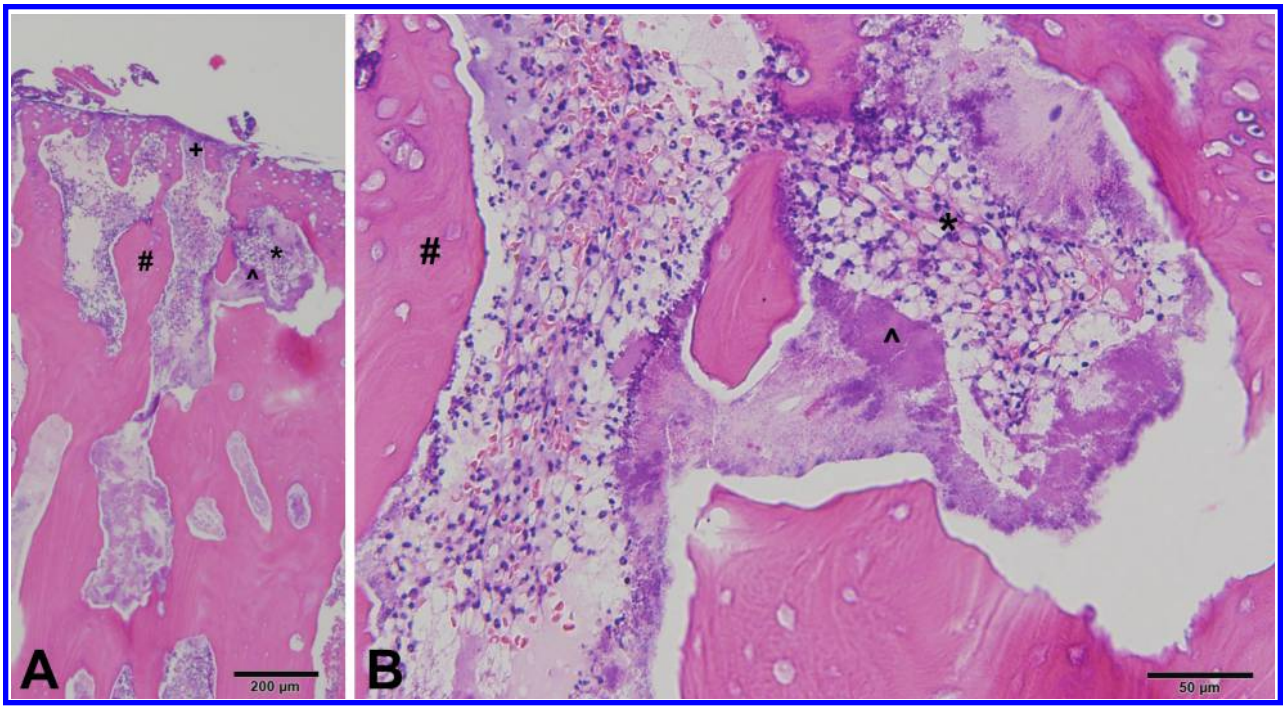

Figure 4—Photomicrographs of a bone fragment section from the TMJ of the dog in Figure 1 at 40X (A) and 200X (B) magnification. The articular cartilage and bone are necrotic, with a marked infiltrate of neutrophils (asterisk) that variably cluster around biofilms (caret) enmeshed within acellular eosinophilic material. Inflammatory cells extend into and disrupt the fibrocartilaginous articular cartilage and primary spongiosa, with loss of proteoglycan matrix and chondrocytes resulting in a pitted, irregular surface nearly devoid of cartilage (plus sign). The bone matrix is bereft of osteocytes within lacunae (pound sign). The trabecular bone margins are severely scalloped, and medullary cavities are expanded by clusters of bacteria. H&E stain; bar = 200 µm (A) and 50 µm (B).

Comments

In this report, advanced imaging with contrast-enhanced CT led to the diagnosis of a chronic bone sequestrum and comminuted fracture of the left condylar and coronoid processes with osteomyelitis, which was confirmed with histopathologic examination and microbial identification. Osteomyelitis typically results from an infectious process and may be classified as hematogenous or posttraumatic, depending on its etiopathogenesis. In dogs and cats, posttraumatic osteomyelitis is more common, occurring through direct inoculation of infectious organisms during traumatic injury or surgery.[1,2] Bacterial infection is usually implicated in dogs with osteomyelitis, with the most commonly identified organisms including *Staphylococcus* spp, followed by *Escherichia coli* and *Streptococcus* spp.[3–7] *Pasteurella* spp, *Pseudomonas* spp, *Proteus* spp, *Serratia* spp, *Klebsiella* spp, *Corynebacterium* spp, and enterococci are other aerobic bacteria that have been reported[7–10]; anaerobes that have been isolated include *Bacteroides* spp, *Nocardia* spp, *Clostridium* spp, *Actinomyces* spp, *Fusobacterium* spp, and *Peptostreptococcus anaerobius*.[2]

Posttraumatic osteomyelitis can be classified as acute or chronic. In acute posttraumatic osteomyelitis, signs are typically apparent within a few days after the traumatic event and include pain, local erythema, and soft tissue swelling, often accompanied by clinical signs of systemic illness.[2,8,11] Chronic posttraumatic osteomyelitis is more common in veterinary patients[2] and is generally a more localized process after acute and systemic clinical signs have subsided. Manifestations of chronic disease may include draining tracts, abscess formation, and recurrent cellulitis.[11]

Diagnostic imaging is an essential part of the evaluation and diagnosis of posttraumatic osteomyelitis. Conventional radiography may be helpful, but it is likely to have inconsistent findings owing to its low diagnostic yield in the maxillofacial region.[12] Detection of bone loss requires a 30% reduction of bone matrix, which typically takes 1 to 2 weeks to become radiographically apparent after infection.[8] Radiography has a reported sensitivity and specificity of 62.5% and 57.1%, respectively, in the detection of osteomyelitis.[13] The radiographic features of osteomyelitis include multifocal osteolysis, sclerosis, irregular periosteal proliferation, peri-implant lucency, and formation of sequestra with or without involucra.[2,11] Computed tomography has been regarded as a more accurate and useful modality for imaging maxillofacial structures because of the complexity of skull anatomy and superimposition of structures that make radiographs challenging to interpret.[12] Compared with radiography, CT can detect osteomyelitis earlier; CT can also provide high-resolution images for comprehensive and detailed evaluation of soft tissues. Additional advantages include identification of foreign material[14] and assessment of changes to bone.[15]

A positive microbial culture result is the current gold standard for diagnosing posttraumatic osteomyelitis. Care should be taken during sample collection to ensure that an uncontaminated, representative sample is obtained.[2] Posttraumatic osteomyelitis warrants aggressive treatment, which may include drainage, debridement, fracture stabilization, removal of implants and foreign material, and sequestrectomy, in addition to appropriate antimicrobial treatment.[2,11,15] One of the primary reasons that antimicrobial treatment alone is usually insufficient, especially in patients with chronic posttraumatic osteomyelitis, is that the distribution of systemically administered antimicrobial agents is often affected by alterations in blood flow, poor local immunity, and presence of sequestra and inflammation, resulting in tissue ischemia. Moreover, biofilms, which often form on sequestra and implants, have increased resistance to antimicrobial agents, making removal of the sequestra or implant the only way to eliminate this type of infection.[2]

The dog of this report initially had clinical signs consistent with acute posttraumatic osteomyelitis including pain and swelling. The dog then developed clinical signs of chronic posttraumatic osteomyelitis including draining tracts. The constellation of findings on contrast-enhanced CT, together with histologic and microbial culture results, confirmed the diagnosis of chronic posttraumatic osteomyelitis by identifying sequestra, necrotic tissue, and abscess and biofilm formation. The dog of this report had no known history of trauma, and CT was essential for determining the cause of chronic posttraumatic osteomyelitis and planning the surgical treatment, which included zygomectomy to access the largest mandibular fragment that included the coronoid process. This case also exemplified the importance of submitting representative samples for microbial culture because of the high incidence of contamination by oral flora when obtaining a swab sample.

Footnotes

a. Isovue-370, Bracco Diagnostics Inc, Singen, Germany.
b. eFilm, Merge Healthcare, Chicago, Ill.
c. eFilm Workstation, version 2.1.0, Merge Healthcare, Chicago, Ill.
d. InVivo5, Anatomage, San Jose, Calif.

References

1. Griffon D. Osteomyelitis. In: Griffon D, Hamaide A, eds. *Complications in small animal surgery.* Ames, Iowa: Wiley Blackwell, 2016;28–33.
2. Robinson D. Osteomyelitis and implant-associated infections. In: Tobias KM, Johnston SA, eds. *Veterinary surgery: small animal expert consult (e-book).* 2nd ed. St Louis: Elsevier Inc, 2017;775–783.
3. Johnson KA. Osteomyelitis in dogs and cats. *J Am Vet Med Assoc* 1994;204:1882–1887.
4. Siqueira EG, Rahal SC, Ribeiro MG, et al. Exogenous bacterial osteomyelitis in 52 dogs: a retrospective study of etiology and in vitro antimicrobial susceptibility profile (2000–2013). *Vet Q* 2014;34:201–204.
5. Caywood DD, Wallace LJ, Braden TD. Osteomyelitis in the dog: a review of 67 cases. *J Am Vet Med Assoc* 1978;172:943–946.

6. Smith CW, Schiller AG, Smith AR. Osteomyelitis in the dog: a retrospective study. *J Am Anim Hosp Assoc* 1978;14:589–592.
7. Walker RD, Richardson DC, Bryant MJ, et al. Anaerobic bacteria associated with osteomyelitis in domestic animals. *J Am Vet Med Assoc* 1983;182:814–816.
8. Cockshutt JR, Sumner-Smith G. Bone infection. In: Sumner-Smith G, ed. *Bone in clinical orthopedics*. Stuttgart, Germany: Thieme, 2002;204–217.
9. Muir P, Johnson KA. Anaerobic bacteria isolated from osteomyelitis in dogs and cats. *Vet Surg* 1992;21:463–466.
10. Johnson KA, Lomas GR, Wood AK. Osteomyelitis in dogs and cats caused by anaerobic bacteria. *Aust Vet J* 1984;61:57–61.
11. Schulz KS, Hayashi K, Fossum TW, et al. Other diseases of bones and joints. In: Fossum TW, ed. *Small animal surgery (e-book)*. 5th ed. Philadelphia: Elsevier Inc, 2018;1309–1312.
12. Bar-Am Y, Pollard RE, Kass PH, et al. The diagnostic yield of conventional radiographs and computed tomography in dogs and cats with maxillofacial trauma. *Vet Surg* 2008;37:294–299.
13. Braden TD, Tvedten HW, Mostosky UV, et al. The sensitivity and specificity of radiology and histopathology in the diagnosis of posttraumatic osteomyelitis. *Vet Comp Orthop Traumatol* 1989;2:98–103.
14. Lamb CR, Pope EH, Lee KC. Results of computed tomography in dogs with suspected wooden foreign bodies. *Vet Radiol Ultrasound* 2017;58:144–150.
15. Seiler G, Rossi F, Vignoli M, et al. Computed tomographic features of skull osteomyelitis in four young dogs. *Vet Radiol Ultrasound* 2007;48:544–549.

Appendix

Clinical history of a 20-month-old English Springer Spaniel during the 6.5 months prior to referral to the Dentistry and Oral Surgery Service of a VMTH because of recurrent extraoral swelling in the caudal left mandibular region and an intraoral draining tract.

Time prior to referral examination (mo)	Clinical signs	Other findings	Treatment
6.5	Reluctance to open mouth 2 weeks after initial evaluation, periodontal treatment, and dental extractions	CBC and serum biochemical analysis revealed monocytosis (1.20 X 10^3 monocytes/µL; reference range, 0.16 X 10^3 monocytes/µL to 1.12 X 10^3 monocytes/µL)	Ampicillin trihydrate (26.8 mg/kg, PO, q 8 h for 7 days); carprofen (1.8 mg/kg, PO, q 12 h for 7 days)
5.5	Recurrence of purulent oral discharge	—	Ampicillin (25.9 mg/kg, PO, q 8 h for 10 days); clindamycin hydrochloride (17.1 mg/kg, PO, q 12 h for 10 days); carprofen (1.9 mg/kg, PO, q 12 h for 30 days)
2	Vomiting, lethargy, shivering, halitosis, left oral cavity draining tract	Culture of fluid from draining tract revealed β-hemolytic *Streptococcus* spp and (unspecified) normal flora*; radiography revealed abnormalities of the left mandibular ramus, left TMJ, and lateral margin of the left condylar process; contrast fistulography revealed contrast medium acccumlation rostral to the left TMJ and in the oral cavity†	Amoxicillin–clavulanic acid (13.8 mg/kg, PO, q 12 h for 10 days)
1	Recheck examination revealed persistent abnormal oral discharge	—	Azithromycin (13.8 mg/kg, PO, q 24 h for 30 days); referral to VMTH

To convert mg/kg to mg/lb, divide by 2.2.
*Susceptibility testing was not performed because of predictable effectiveness of the recommended antimicrobials. †**See** text for details.
— = Not applicable.